Regular article

Toxicoproteomic analysis of a mouse model of nonsteroidal anti-inflammatory drug-induced gastric ulcers

Kaname Ohyama[a,b]*, Akina Shiokawa[a], Kosei Ito[b,c], Ritsuko Masuyama[c], Tomoko Ichibangase[d], Naoya Kishikawa[a], Kazuhiro Imai[d], and Naotaka Kuroda[a]

[a]Department of Environmental and Pharmaceutical Sciences, Graduate School of Biomedical Sciences, Nagasaki University, Nagasaki, Japan

[b]Nagasaki University Research Centre for Genomic Instability and Carcinogenesis (NRGIC)

[c]Department of Cell Biology, Graduate School of Biomedical Sciences, Nagasaki University, Nagasaki, Japan

[d]Research Institute of Pharmaceutical Sciences, Musashino University, Nishitokyo-shi, Tokyo, Japan

*Corresponding author. Department of Environmental and Pharmaceutical Sciences, Graduate School of Biomedical Sciences, Nagasaki University, 1-14 Bunkyo-machi, Nagasaki 852-8521, Japan.

Tel/Fax: +81-95-819-2446; E-mail: k-ohyama@nagasaki-u.ac.jp

Abbreviations: Dic, diclofenac; ER, endoplasmic reticulum; FD-LC-MS/MS, fluorogenic derivatization-liquid chromatography-tandem mass spectrometry; GRP78, 78 kDa glucose-regulated protein; HSP27, heat shock protein beta-1; MAPK, mitogen-activated protein kinase; NSAIDs, nonsteroidal anti-inflammatory drugs

Abstract

Nonsteroidal anti-inflammatory drugs (NSAIDs) are valuable agents; however, their use has been limited by their association with mucosal damage in the upper gastrointestinal tract. NSAIDs inhibit cyclooxygenase and consequently block the synthesis of prostaglandins, which have cytoprotective effects in gastric mucosa; these effects on prostaglandins have been thought to be major cause of NSAID-induced ulceration. However, studies indicate that additional NSAID-related mechanisms are involved in formation of gastric lesions. Here, we used a toxicoproteomic approach to understand cellular processes that are affected by NSAIDs in mouse stomach tissue during ulcer formation. We used fluorogenic derivatization-liquid chromatography-tandem mass spectrometry (FD-LC-MS/MS) - which consists of fluorogenic derivatization, separation and fluorescence detection by LC, and identification by LC-tandem mass spectrometry - in this proteomic analysis of pyrolic stomach from control and diclofenac (Dic)-treated mice. FD-LC-MS/MS results were highly sensitive; 10 differentially expressed proteins were identified, and all 10 were more highly expressed in Dic-treated mice than in control mice. Specifically, expression levels of 78 kDa glucose-regulated protein (GRP78), heat shock protein beta-1 (HSP27), and gastrin were more than 3-fold higher in Dic-treated mice than in control mice. This study represents a first step to ascertain the precise actors of early NSAID-induced ulceration.

Keywords: nonsteroidal anti-inflammatory drugs; gastric ulceration; fluorogenic derivatization-liquid chromatography tandem mass spectrometry; toxicoproteomics

Introduction

Nonsteroidal anti-inflammatory drugs (NSAIDs) are some of the most prescribed drugs worldwide; however, their use has been limited by their association with mucosal injury to the upper gastrointestinal tract. As many as 25% of chronic NSAIDs users may develop ulcer disease, and 2-4% of the ulcers may bleed or perforate [1, 2]. In the United States, these gastrointestinal events result in more than 100,000 hospital admissions annually and between 7,000 and 10,000 deaths [3]. NSAIDs inhibit cyclooxygenase (COX) and consequently block the synthesis of prostaglandins, which have cytoprotective effects in gastric mucosa; this has been thought to be the major mechanism of the NSAID-induced ulceration [4]. However, there is some evidence that COX inhibition is not the sole mechanism by which NSAIDs cause gastrotoxic effects, suggesting that formation of gastric lesions result from other NSAID-mediated processes [5].

Proteomics is the large-scale study of gene expression at the protein level, and it provides information on dynamic cellular activity. As an integration of proteomics, toxicology, and bioinformatics, toxicoproteomics mainly focuses on changes in protein expression in cells or tissues following or during exposure to toxins, including pharmaceuticals [6, 7]. Therefore, toxicoproteomic analysis of stomach tissue is a good approach to understand the cellular processes that result in NSAID-induced gastric ulcer; however, such analysis has not yet been performed.

In proteomic studies, comparative expression profiling of proteins has usually been performed using two-dimensional electrophoresis (2-DE). However, the 2-DE method has

some drawbacks with regard to the reproducibility of the data. Imai and colleagues developed an easily reproducible and highly sensitive proteomic approach, fluorogenic derivatization-liquid chromatography-tandem mass spectrometry (FD-LC-MS/MS) [8-10]. This method involves fluorogenic derivatization of proteins, followed by high-performance liquid chromatography (LC) of the derivatized proteins, isolation of those proteins that are differentially expressed in treatment groups, enzymatic digestion of the isolated proteins, and identification of the isolated proteins via LC-tandem MS using a database-searching algorithm. This method enables highly sensitive detection of proteins due to the fluorogenic derivatization which utilizes a non-fluorescent reagent to yield highly fluorescent products.

The aim of this study was to use FD-LC-MS/MS to understand the cellular processes in gastric tissues that are affected by administration of diclofenac (Dic) which is one of NSAIDs most frequently used in clinical setting. To our knowledge, this report describes the first comprehensive analysis of differential protein expression in stomach tissue using a mouse model of NSAID-induced gastric lesions.

Material and methods

Animal treatment and tissue processing

Male C57BL/6J mice (9 weeks old) were purchased from Japan SLC (Nagasaki, Japan) and acclimatized for 1 week before experiment. Animal care and experimental procedures were performed in accordance with the Guide for the Care and Use of Laboratory Animals (National Institute of Health) with approval from the Institutional Animal Care and

Use Committee of the Graduate School of Biomedical Sciences, Nagasaki University. Mice received a single intraperitoneal injection of Dic (0.1 g/kg dissolved in saline, Tokyo Chemical Industry, Tokyo, Japan) or of saline alone, as a negative control. The animals were deprived of food but had free access to tap water for 24 h prior Dic or saline injection. Pyloric stomach samples for FD-LC-MS/MS analysis were isolated from each mouse 6 h after saline or Dic was administered. Each sample was immediately rinsed with phosphate buffer saline and frozen at -196°C. Samples were homogenized using the Frozen Cell Crasher (Microtec Co., Ltd., Chiba, Japan). Four mice were used in each experimental group.

Histological staining of NSAID-induced gastric lesions

The stomachs were fixed with 10% neutral buffered formalin, embedded in paraffin, and then cut into sections (4 μm thick) at 1-mm horizontal intervals from the fundus to the pylorus; these sections were stained with hematoxylin-eosin (H&E). We examined the stomach tissues collected at 6 h and 24 h after treatment.

Extraction of proteins and determination of total protein concentration

Each sample of homogenized pyloric stomach tissue (50 mg) was suspended in 250 μl of 10 mM 3-[(3-cholamidopropyl)-dimethylammonio] propanesulfonate (CHAPS) solution (Dojindo Laboratories, Kumamoto, Japan), and the homogenates were centrifuged at 5000 *g* for 15 min at 4°C. The supernatant of each sample was then collected and stored as the soluble fraction at -80°C until use. The total protein content of each supernatant sample was

determined using the Quick Start Bradford Protein assay kit (Bio-Rad Laboratory, Hercules, CA, USA) and bovine serum albumin as a protein standard according to the manufacture's instructions. After determination of total protein content in the soluble fractions, the supernatant was diluted with CHAPS solution to a concentration of 4.0 mg total protein/ml and used as a starting protein sample.

FD-LC-MS/MS method

A 10-μl volume of sample was combined with 85 μl of a mixture of 0.83 mM tris(2-carboxyethyl)phosphine hydrochloride (Tokyo Chemical Industry), 3.33 mM ethylenediamine-*N,N,N',N'*-tetraacetic acid (Dojindo Laboratories), and 16.6 mM CHAPS in 6 M guanidine hydrochloride buffer solution (pH 8.7, Tokyo Chemical Industry). Then, this sample was subsequently mixed with 5 μl of 140 mM 7-chloro-*N*-[2-(dimethylamine)ethyl]-2,1,3-benzoxadiazole-4-sulfonamide (DAABD-Cl, Tokyo Chemical Industry), which is the fluorogenic derivatization reagent, in acetonitrile (Merck KGaA, Darmstadt, Germany). After each reaction mixture was incubated in a 50°C water bath for 5 min, 3 μl of 20% trifluoroacetic acid (TFA, Nacalai Tesque, Kyoto, Japan) was added to each sample to stop the derivatization reaction. A portion (20 μl) of each reaction mixture (8 μg protein) was injected into the HPLC-fluorescence detection system consisting of a Shimadzu Prominence series HPLC system (Kyoto, Japan), a fluorescence detector (Shimadzu RF-10 A_xL; λex. 395 nm; λem. 505 nm), and a Sunniest C8-WP column (ChromaNik Technologies, Tokyo, Japan) at a flow rate of 0.55 ml/min and a column

temperature of 60°C. The mobile phase consisted of 0.1% TFA in (A) water and (B) acetonitrile. The gradient elution was established with the following condition: 10% B held for 10 min; to 18% B in 30 min; to 32% B in 130 min; to 37% B in 215 min; to 42% B in 411 min; to 46% B in 486 min; to 52% B in 569 min; to 65% B in 600 min; to 70% B in 610 min. Corresponding peak heights were compared to identify differential protein profiles. Each subject protein in eluant recovered from the above HPLC system was concentrated into a 5-μl volume under reduced pressure, and these concentrates were used in subsequent identification procedures. The residue was diluted with 240 μl of 50 mM ammonium bicarbonate solution (pH 7.8) (Nacalai Tesque), 5 μl of 10 mM calcium chloride (Nacalai Tesque), and 5 μl of 20 ng/μl trypsin (Promega, Wisconsin, WI, USA), and the resultant mixtures were incubated for 6 h at 37°C. Each mixture was then concentrated to 20 μl under reduced pressure. Each peptide mixture was subjected to an LC-electrospray ionization-tandem mass spectrometer (LTQ XL, Thermo Fisher Scientific, Waltham, MA, USA) equipped with the custom nanoLC system consisting of an LC pump (LC-20AD, Shimadzu) with LC flow splitter (Accurate, Dionex, Sunnyvale, CA, USA) and an HCT PAL autosampler (CTC Analytics, Zwingen, Switzerland). The sample was loaded onto a precolumn (300 μm i.d. x 5.0 mm, L-C-18, Chemicals and Evaluation and Research Institute, Tokyo, Japan) in the injection loop and washed using 0.1% TFA in 2% acetonitrile. Peptides were separated and ion-sprayed into MS by a nano HPLC column (75 μm i.d. x 15 cm, Acclaim PepMap100C18, 3 μm, Dionex) with a spray voltage from 1.5 to 2.5 kV. Separation was performed, employing a gradient from 5 to 50% mobile phase B (0.1% formic acid in 90% acetonitrile) over a period of 30 min

(mobile phase A: 0.1% formic acid); 50 to 100% mobile phase B in 30.1 min; 100% mobile phase B held for 10 min. The mass spectrometer was configured to optimize the duty cycle length with the quality of data acquired by progressing from a full scan of the sample to three tandem MS scans of the three most intense precursor masses (as determined by Xcaliber® software [Thermo Fisher Scientific] in real time). The collision energy was normalized to 35%. All the spectra were measured with an overall mass/charge ratio range of 400-1500. The transfer capillary temperature was set at 200°C. MS/MS data were extracted using Proteome Discoverer 1.2 (Thermo Fisher Scientific). Spectra were searched against a murine subdatabase from the public non-redundant protein database, International Protein Index version 3.82, maintained by The European Bioinformatics Institute with the following search parameters: mass type, monoisotopic precursor and fragments; enzyme, trypsin (KR); enzyme limits, full enzymatic cleavage allowing up to two missed cleavages; peptide tolerance, 1.2 Da; fragment ion tolerance, 0.8 Da; ion and ion series calculated, B and Y ions; static modification, C (fluorogenic derivatization); differential modifications, M (oxidation), N and Q (deamidation). Initial searching results were filtered with the following parameter: single, double, and triple charge peptides with a correlation factor (XCorr) greater than 1.6, 2.0, and 2.4, respectively. Ubiquitous keratins and trypsin were excluded as potential matches.

Statistical analysis

Differences in peak heights between control and Dic-treated mice were determined

by unpaired two-tailed *Student*'s t-test. $P < 0.05$ was considered to be significant.

Results and discussion

Development of a mouse model of NSAID-induced gastric injury

Our first aim was to develop a mouse model of NSAID-induced gastric ulcer. A single dose of Dic induced multiple ulcers and erosions in mouse stomach mucosa within less than 24 h (Fig. 1). Following Dic injection, the damage observed after 24 h was more severe and wider than that observed after 6 h. The lesions were most abundant in the pyloric region; only a few lesions were evident in the body or fundic regions of stomachs, and the duodenum was free of any apparent ulceration. NSAID-induced ulcerations in clinical settings are most frequently found in the pyloric stomach [11, 12], and our finding was consistent with this observation. Therefore, the mouse model used here was adequate for our subsequent toxicoproteomic study, and this study focused on profiling differential protein expression in the pyloric stomach. The number of ulcers in mouse intestine was reported not to be significantly changed at longer than 6 h post-treatment [13]. Also, understanding the pathogenesis during early ulcer formation is effective for the prevention; therefore, we decided to collect tissue samples at 6 h after administration of Dic or saline for the proteomic analysis.

Differential profiling and protein identification

Typical chromatograms from FD-LC of control and Dic-dosing samples are depicted

in Fig. 2. The height of each peak indicates the expression level of an individual protein. Expression of 10 proteins differed significantly between Dic-treated and saline-treated mice ($P < 0.05$; Table 1); the peaks representing these proteins are numbered in Fig. 2. Each differentially expressed protein was more highly expressed in the Dic group than in the control group. The expression of 78 kDa glucose-regulated protein (GRP78, peak no. 7), heat shock protein beta-1 (HSP27, peak no. 6), and gastrin (peak no. 1) was more 3-fold higher in the Dic-dosing group than in the control group.

Endoplasmic reticulum (ER) is an organelle that participates in protein synthesis, folding and modification of membrane and secretory proteins, and maintenance of cellular calcium homeostasis. The conditions or stresses that interfere with ER function are called ER stress [14]. Chemical toxins and oxidative stress can all disrupt ER function and result in ER stress [15-17]. Cells experiencing ER stress initiate the ER stress response, which facilitates protein refolding and prevents aggregation of irreversible misfolding proteins. GRP78 (peak no. 7) is a resident ER protein and a member of the HSP70 family of charperones; GRP78 binds to hydrophobic patches of nascent polypeptides in ER to prevent protein disaggregation. GRP78 also plays a key role in ER stress-induced apoptosis signaling. Cells initially adapt to ER stress by inducing ER-resident stress proteins such as GRP78 and GRP94 [14, 18, 19]; however, if this adaption is not sufficient, ER-initiated apoptosis signaling and proteins such as CCAAT/enhancer-binding protein homologous protein (CHOP), c-Jun-N-terminal kinase (JNK), and caspase-12 are activated [20-22]. GRP78 acts as an apoptotic regulator. Evidence shows that the overexpression of GRP78

might prevent ER stress-induced cell death by reducing levels of CHOP and inducing formation of a complex that includes GRP78, caspase-7, and caspase-12 [23-26]. Tsutsumi *et al*. reported that induction of apoptosis by NSAIDs via a CHOP pathway is involved in NSAID-induced gastric lesion formation [27, 28]. They also found that GRP78 was overexpressed in cells exposed to NSAIDs, and they proposed that GRP78 could be developed as an antiulcer drug because it suppresses apoptosis [28].

The heat shock protein (HSP) family has long been associated with a generalized cellular stress response, particularly in terms of chaperoning misfolded proteins. In addition to this well-documented function, HSP27 (peak no. 6) may mediate cell survival directly. Several studies indicate that HSP27 diminishes the activation of procaspase-9 by inhibiting the interaction between procaspase-9 and cytochrome *c*, thus preventing the proper formation of the apoptosome complex [29, 30]. Furthermore, HSP27 can inhibit caspase-3 activity by interacting with the procaspase-3 molecule [29, 31]. These observations are consistent with a scenario in which HSP27 inhibits apoptosis by targeting the pathways downstream of the mitochondrial release of cytochrome *c*. Therefore, the overexpression of HSP27 that we observed may indicate that HSP27 expression was elevated for counteracting or suppressing NSAID-induced apoptosis.

Gastrin (peak no. 1) was originally identified as a potent stimulant of gastric acid secretion and the increased acid secretion may contribute to ulcer formation. Mitogen-activated protein kinase (MAPK) pathways are important signal transduction cascades that link extracellular stimuli to intracellular responses. Among the different

MAPK pathways described in the literature (e.g., extracellular signal-regulated kinase pathway, JNK pathway, and p38-MAPK pathway), JNK and p38-MAPK are associated with cellular apoptosis, and p38-MAPK signaling is reportedly necessary for CHOP induction and apoptosis [32]. Gastrin activates the p38-MAPK pathway [33, 34]; therefore, gastrin may activate CHOP or enhance activated CHOP and, thereby, cause in NSAID-induced ulceration. On the other hand, HSP27 is reportedly phosphorylated by several kinases downstream of p38-MAPK [35, 36], and this phosphorylation is induced by ER stress [37]. Recently, Ock *et al*. reported that indomethacin-induced cytotoxicity was accompanied by HSP27 phosphorylation in cell culture experiments and that HSP27 dephosphorylation protected stomach tissue from indomethacin-induced damage in an animal experiment [38]. Furthermore, the activation of p38-MAPK by gastrin can enhance the cytotoxic effects of phosphorylated HSP27. In these contexts, inhibiting expression or activity of gastrin may help prevent NSAID-induced gastric damage.

Calponin-1 (peak no. 4) is known to activate protein kinase C (PKC) autophosphorylation [39], and PKC is able to phosphorylate Raf, an upstream activator of MAPK/ERK. Calponin-1 may up-regulate MAPK by promoting the formation of a signaling complex comprising PKC, Raf, MAPK, and ERK.

We found that glutathione *S*-transferase (GST)-α (peak no. 10) expression was 1.9-fold higher in the Dic group than in the control group. GST-α may have been overexpressed because it functions in a detoxification system against chemical toxins. Similarly, van Lieshout reported that NSAIDs increased GST-α expression in the upper

digestive tract in rats [40].

In this study, COX enzymes were not found to be altered by administration of Dic. This may be because NSAIDs action is not directed towards the transcription or translation of the COX genes but only to the enzymatic activity of the proteins [41, 42].

In summary, in order to understand the cellular processes that are altered in a mouse model of NSAID-induced gastric ulceration, FD-LC-MS/MS was applied to differential proteomic analysis of pyloric stomach tissues from saline- and Dic-treated mice. Using this toxicoproteomic method, we identified significantly altered and elevated expression of 10 proteins. Of these proteins, three (GRP78, HSP27, and gastrin) are involved in cellular apoptosis, which is supposed to partially cause for gastric lesions; moreover, expression of these three was more highly elevated than that of the other 7 differentially expressed proteins. Our hypothetical model of NSAID-induced gastric lesion formation is summarized in Fig. 3. This study represents a first step to ascertain the precise actors of early NSAID-induced ulceration. Further analyses of GRP78, HSP27, and gastrin are necessary to determine if they are a potential target for protective intervention against the ulceration.

Acknowledgements

This work was supported by the Special Coordination Funds for Promoting Science and Technology of the Ministry of Education, Culture, Sports, Science and Technology (MEXT). This work was supported by The Shimabara Science Promotion Foundation. The authors thank ChromaNik Technologies for kindly supplying Sunniest C8-WP column.

References

[1] F.E. Silverstein, G. Faich, J.L. Goldstein, et al., Gastrointestinal toxicity with celecoxib vs. nonsteroidal anti-inflammatory drugs for osteoarthritis and rheumatoid arthritis: the CLASS study: A randomized controlled trial. Celecoxib Long-term Arthritis Safety Study, JAMA 284 (2000) 1247-1255.

[2] F.L. Lanza, F.K.L Chan, E.M.M. Quigley, Guidelines for prevention of NSAID-related ulcer complications, Am. J. Gastroenterol. 104 (2009) 728-738.

[3] G. Singh, Recent consideration in nonsteroidal anti-inflammatory drug gastropathy, Am. J. Med. 105 (1998) 31S-38S.

[4] R. Langenbach, S.G. Morham, H.F. Tiano, et al., Prostaglandin Synthase 1 gene disruption in mice reduces arachidonic acid-induced inflammation and indomethacin-induced gastric ulceration, Cell 83 (1995) 483-492.

[5] C. Musumba, D.M. Pritchard, M. Pirmohamed, Cellular and molecular mechanisms of NSAID-induced peptic ulcer, Aliment. Pharmacol. Ther. 30 (2009) 517-531.

[6] Y. Ge, R.J. Preston, R.D. Owen, Toxicoproteomics and its application to human health risk assessment, Proteomics Clin. Appl. 1 (2007) 1613-1624.

[7] L.R. Bandara, S. Kennedy, Toxicoproteomics-a new preclinical tool, Drug Discov. Today 7 (2002) 411-418.

[8] M. Masuda, C. Toriumi, T. Santa, T., et al., Fluorogenic derivatization reagents suitable for isolation and identification of cystein-containing proteins utilizing high-performance liquid chromatography-tandem mass spectrometry, Anal. Chem. 76 (2004) 728-735.

[9] T. Ichibangase, K Moriya, K. Koike, et al., A proteomic method revealing disease-related proteins in livers of hepatitis-infected mouse model, J. Proteome Res. 6 (2007) 2841-2849.

[10] K. Ohyama, M. Tomonari, T. Ichibangase, et al., A toxicoproteomic study on cardioprotective effects of pre-administration of docetaxel in a mouse model of adriamycin-induced cardiotoxicity, Biochem. Pharmacol. 80 (2010) 540-547.

[11] F.L. Lanza, Endoscopic studies of gastric and duodenal injury after the use of ibuprofen, aspirin, and other nonsteroidal anti-inflammatory agents, Am. J. Med. 13 (1984) 19-24.

[12] J.F. Fries, S.R. Miller, P.W. Spitz, et al., Toward an epidemiology of gastropathy associated with nonsteroidal anti-inflammatory drug use, Gastroenterology 96 (1989) 647-655.

[13] V. Ramirez-Alcantara, A. LoGuidice, U.A. Boelsterli, Protection from diclofenac-induced small intestinal injury by the JNK inhibitor SP600125 in a mouse model of NSAID-associated enteropathy, Am. J. Physiol. Gastrointest. Liver. Physiol. 297 (2009) G990-G998.

[14] R.J.Kaufman, Stress signaling from the lumen of endoplasmic reticulum: coordination of gene transcriptional and translational controls, Genes Dev. 13 (1999) 1211-1233.

[15] Y. Kozutsumi, M. Segal, K. Normington, et al., The presence of malfolded proteins in the endoplasmic reticulum signals the induction of glucose-regulated proteins, Nature 322 (1988) 462-464.

[16] K. Mori, Tripartile management of unfolded proteins in the endoplasmic reticulum, Cell 101 (2000) 451-454.

[17] R.V. Rao, H.M. Ellerby, D.E. Bredesen, Coupling endoplasmic reticulum stress to the cell death program, Cell Death Differ. 11 (2004) 372-380.

[18] S.K. Wooden, L.J. Li, D. Navarro, et al., Transactivation of the grp78 promoter by malfolded proteins, glycosylation block, and calcium ionophore is mediated through a proximal region containing a CCAT motif which interacts with CTF/NF-I, Mol. Cell. Biol. 11 (1991) 5612-5623.

[19] H. Liu, R.C. Bowes III, B. van de Water, et al., Endoplasmic reticulum chaperones GRP78 and calreticulin prevent oxidative stress, Ca^{2+} disturbances, and cell death in renal epithelial cells J. Biol. Chem. 272 (1997) 21751-21759.

[20] S. Oyadomari, M. Mori, Roles of CHOP/GADD153 in endoplasmic reticulum stress, Cell Death Differ. 11 (2004) 381-389.

[21] F. Urano, X. Wang, A. Bertolotti, et al., Coupling of stress in the ER to activation of JNK protein kinases by transmembrane protein kinase IRE1, Science 287 (2000) 664-666.

[22] N. Morishima, K. Nakanishi, H. Takenouchi, et al., An endoplasmic reticulum stress-specific caspase cascade in apoptosis. Cytochrome *c*-independent activation of caspase-9 by caspase-12, J. Biol. Chem. 277 (2002) 34287-34294.

[23] J.A. Morris, A.J. Dorner, C.A. Edwards, et al., Immunoglobulin binding protein (Bip) function is required to protect cells from endoplasmic reticulum stress but is not required for the secretion of selective proteins, J. Biol. Chem. 272 (1997) 4327-4334.

[24] T. Nakagawa, H. Zhu, N. Morishima, et al., Caspase-12 mediates endoplasmic reticulum-specific apoptosis and cytotoxicity by amyloid-beta, Nature 403 (2000) 98-103.

[25] H.Y. Fu, T. Minamino, O. Tsukamoto, et al., Overexpression of endoplasmic reticulum-resident chaperone attenuates cardiomyocyte death induced by proteasome inhibition, Cardiovasc. Res. 79 (2008) 600-610.

[26] M.S. Gorbatyuk, T. Knox, M.M. LaVail, et al., Restoration of visual function in P23H rhodopsin transgenic rats by gene delivery of Bip/Grp78, Proc Natl Acad Sci USA 107 (2010) 5961-5966.

[27] W. Tomisato, S. Tsutsumi, T. Hoshino, et al., Role of direct cytotoxic effects of NSAIDs in the induction of gastric lesions, Biochem. Pharmacol. 67 (2004) 575-585.

[28] S. Tsutsumi, T. Gotoh, W. Tomisato, et al., Endoplasmic reticulum stress response is involved in nonsteroidal anti-inflammatory drug-induced apoptosis, Cell Death Differ. 11 (2004) 1009-1016.

[29] C.G. Concannon, S. Orrenius, A. Samali, Hsp27 inhibits cytochrome *c*-mediated caspase activation by sequestering both pro-caspase-3 and cytochrome *c*, Gene Expr. 9 (2001) 195-201.

[30] C. Garrido, J.M. Bruey, A. Fromentin, et al., HSP27 inhibits cytochrome *c*-dependent activation of procaspase-9, FASEB J. 13 (1999) 2061-2070.

[31] P. Pandey, R. Farber, A. Nakazawa, et al., Hsp27 functions as a negative regulator of cytochrome *c*-dependent activation of procaspase-3, Oncogene 19 (2000) 1975-1981.

[32] T. DeVries-Seimon, Y. Li, P.M. Yao, et al., Cholesterol-induced macrophage apoptosis requires ER stress pathways and engagement of the type A scavenger receptor, J. Cell Biol. 171 (2005) 61-73.

[33] S. Dehez, L. Daulhac, A. Kowalski-Chauvel, et al., Gastrin-induced DNA synthesis requires p38-MAPK activation via PKC/Ca^{2+} and Src-dependent mechanisms, FEBS Lett. 496 (2001) 25-30.

[34] D. Subramaniam, S. Ramalingam, R. May, et al., Gastrin-mediated interleukin-8 and cyclooxygenase-2 gene expression: Differential transcriptional and posttranscriptional mechanism, Gastroenterology 134 (2008) 1070-1082.

[35] D. Stokoe, D.G. Campbell, S. Nakielny, et al., MAPKAP kinase-2; a novel protein kinase activated by mitogen-activated protein kinase, EMBO J. 278 (1992) 3985-3994.

[36] L. New, Y. Jiang, M. Zhao, et al., PRAK, a novel protein kinase regulated by the p38 MAP kinase, EMBO J. 17 (1998) 3372-3384.

[37] H. Ito, I. Iwamoto, Y. Inaguma, et al., Endoplasmic reticulum stress induces the phosphorylation of small heat shock protein, Hsp27. J. Cell Biochem. 95 (2005) 932-941.

[38] C.Y. Ock, Y.J. Lim, Y.J. Kim, et al., Acid pump antagonist-provoked HSP27 dephosphorylation and accentuation rescues stomach from indomethacin-induced damages, J. Dig. Dis. 12 (2011) 71-81.

[39] B. Leinwever, A.M. Parissenti, C. Gallant, et al., Regulation of protein kinase C by the cytoskeletal protein calponin, J. Biol. Chem. 275 (2000) 40329-40336.

[40] E.M.M. van Lieshout, D.M. Tiemessen, W.H.M. Peters, et al., Effects of nonsteroidal anti-inflammatory drugs on glutathione *S*-transferases of the rat digestive tract, Carcinogenesis 18 (1997) 485-490.

[41] M. Barrios-Rodiles, K. Keller, A. Belley, et al., Nonsteroidal antiinflammatory drugs

inhibit cyclooxygenase-2 enzyme activity but not mRNA expression in human macrophages, Biochem. Biophys. Res. Commun. 225 (1996) 896-900.

[42] S.E. Elliott, W. McKnight, G. Cirino, et al., A nitric oxide-releasing nonsteroidal anti-inflammatory drug accelerates gastric ulcer healing in rats, Gastroenterology 109 (1995) 524-530.

Figure captions

Fig. 1 Representative Dic-induced gastric ulcers in the pyloric region at 6 h and 24 h after treatment in C57BL/6J. H&E staining was performed as described in Material and methods section.

Fig. 2 Representative chromatograms of proteins derivatized with DAABD-Cl in mouse pyloric stomach. The upper and lower chromatograms were obtained with samples from saline-treated and Dic-treated mice, respectively. The peaks of differentially expressed proteins are numbered in each chromatogram.

Fig. 3 Hypothetical model of NSAID-induced gastric injury. NSAIDs induce ER stress. Excess ER stress, which cannot be fully ameliorated by chaperones, activates an ER-induced apoptosis signal that leads to activation of p38-MAPK, JNK, and CHOP. GRP78 and HSP27 inhibit CHOP and caspases-3, -9, and -12. Activation of p38-MAPK by gastrin results in acceleration of apoptosis signaling and phosphorylation of HSP27. GST-α detoxifies NSAIDs.

Table 1 List of proteins identified by FD-LC-MS/MS method

Peak number[a]	Protein name	Dic-dosing/control ratio[b]	Molecular mass (kDa)	SEQUEST score	Peptide hit	Coverage by mass	Accession[c]
1	Gastrin	3.7**	11.6	6.85	2	22.77	IPI00319752.1
2	Actin	2.2*	41.7	15.86	3	25.60	IPI00110850.1
3	40S ribosomal protein S20-like	1.7*	12.9	33.55	5	37.39	IPI00987717.1
4	Calponin-1	2.2*	29.1	15.63	4	16.34	IPI00228258.1
5	Aminoacyl tRNA synthase complex-interacting multifunctional protein 1	2.7*	35.1	2.24	1	33.00	IPI00006252.3
6	Heat shock protein beta-1 (HSP27)	4.2**	19.4	21.47	6	38.86	IPI00623819.1
7	78 kDa glucose-regulated protein (GRP78)	5.2**	72.4	55.53	15	23.21	IPI00319992.1
8	ADP/ATP translocase2	2.0**	32.9	5.36	2	7.38	IPI00127841.3
9	Phosphoglycerate kinase 1	2.3**	44.5	54.58	8	21.58	IPI00555069.3
10	Glutathione S-transferase A4 (GST-α)	1.9**	25.5	38.49	4	26.13	IPI00323911.3

[a]Peak numbers correspond to those in Fig. 2. [b]Dic-dosing/control ratio: the ratio of the amount of a protein in the Dic group relative to that in the control group. [c]IPI number is simply a series of digits that are assigned consecutively to each sequence processed by the International Protein Index. Significant differences between the control and Dic groups are indicated by * ($P \leq 0.05$) or ** ($P \leq 0.01$).

Fig. 1

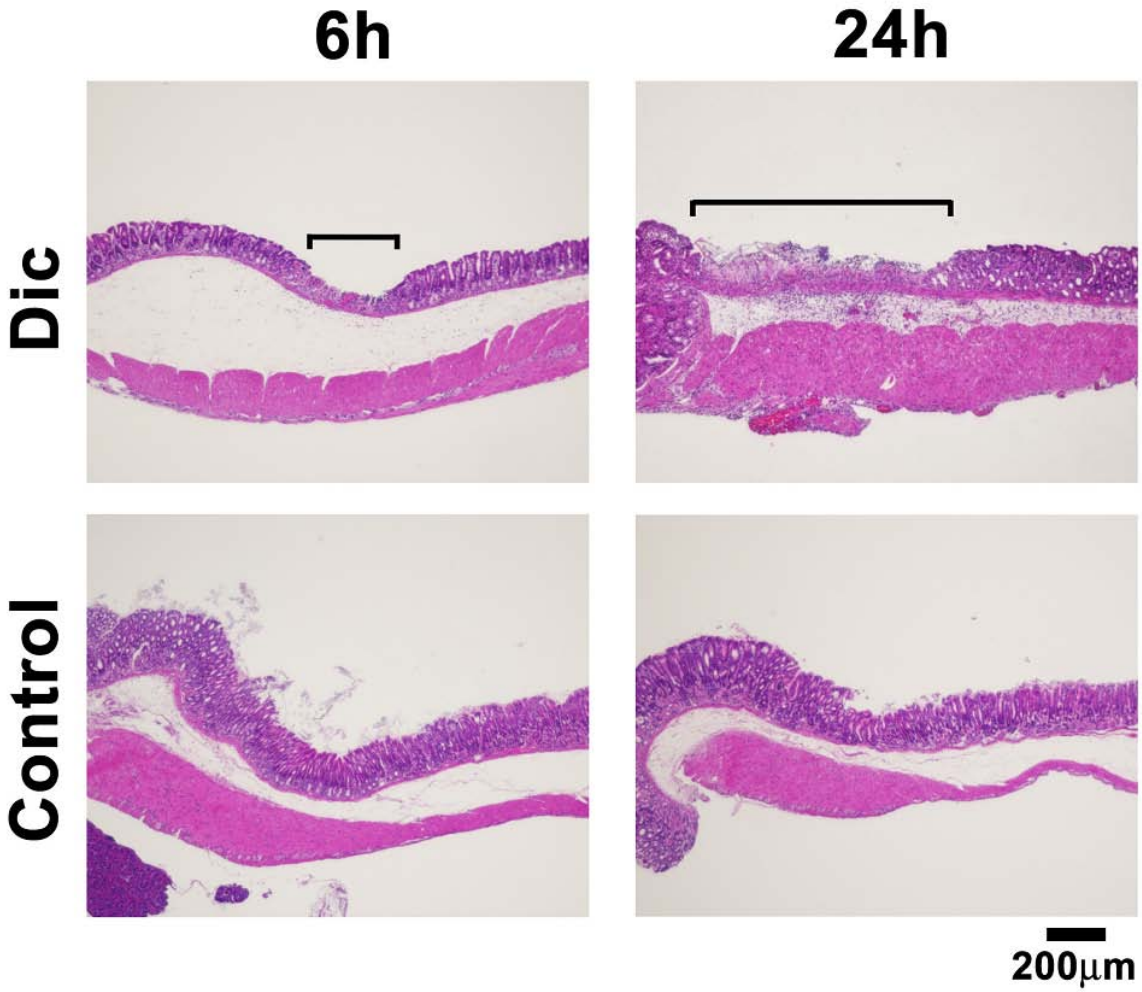

Fig. 2

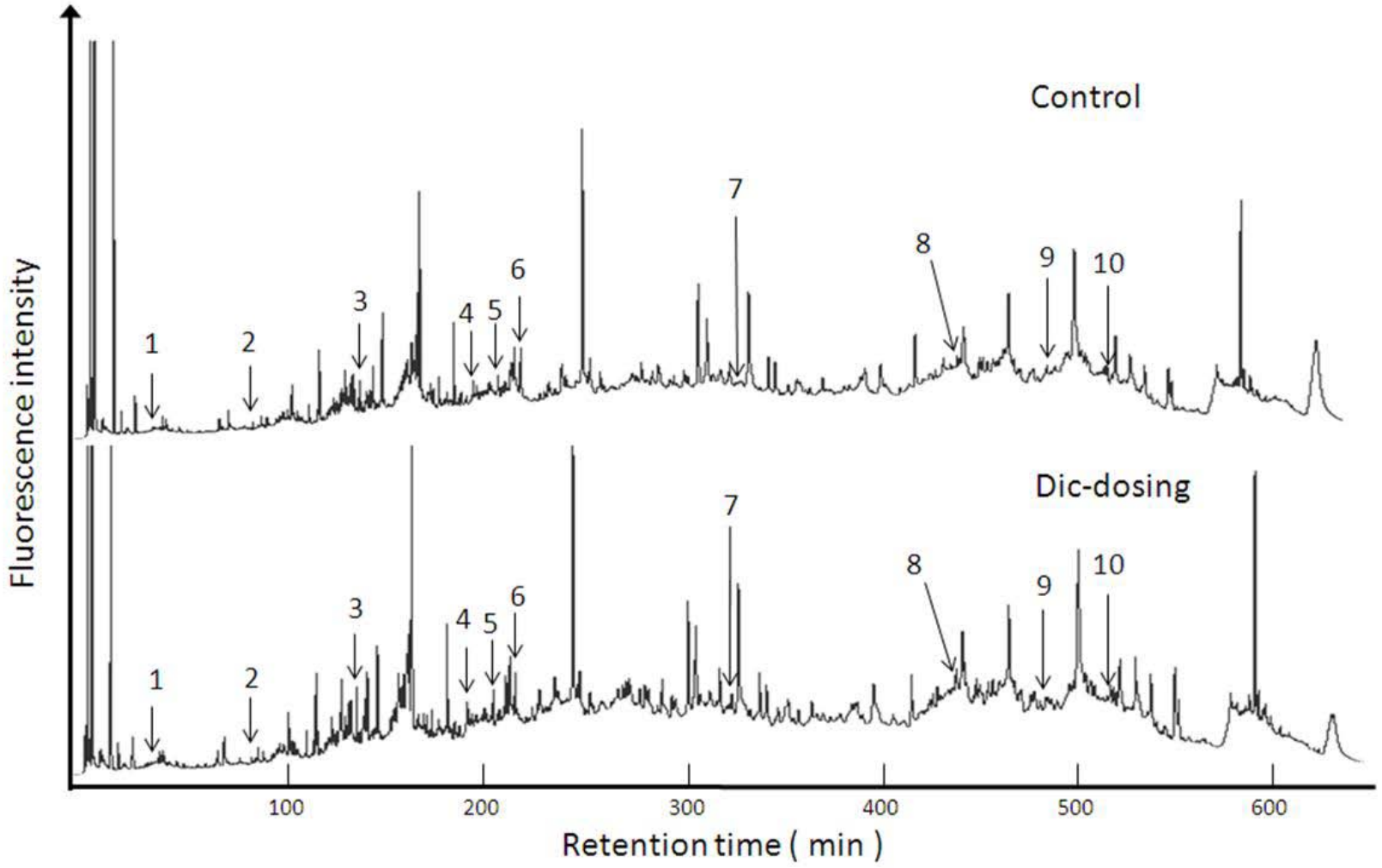
Control
Dic-dosing
Fluorescence intensity
Retention time (min)
100
200
300
400
500
600
1
2
3
4
5
6
7
8
9
10

Fig. 3

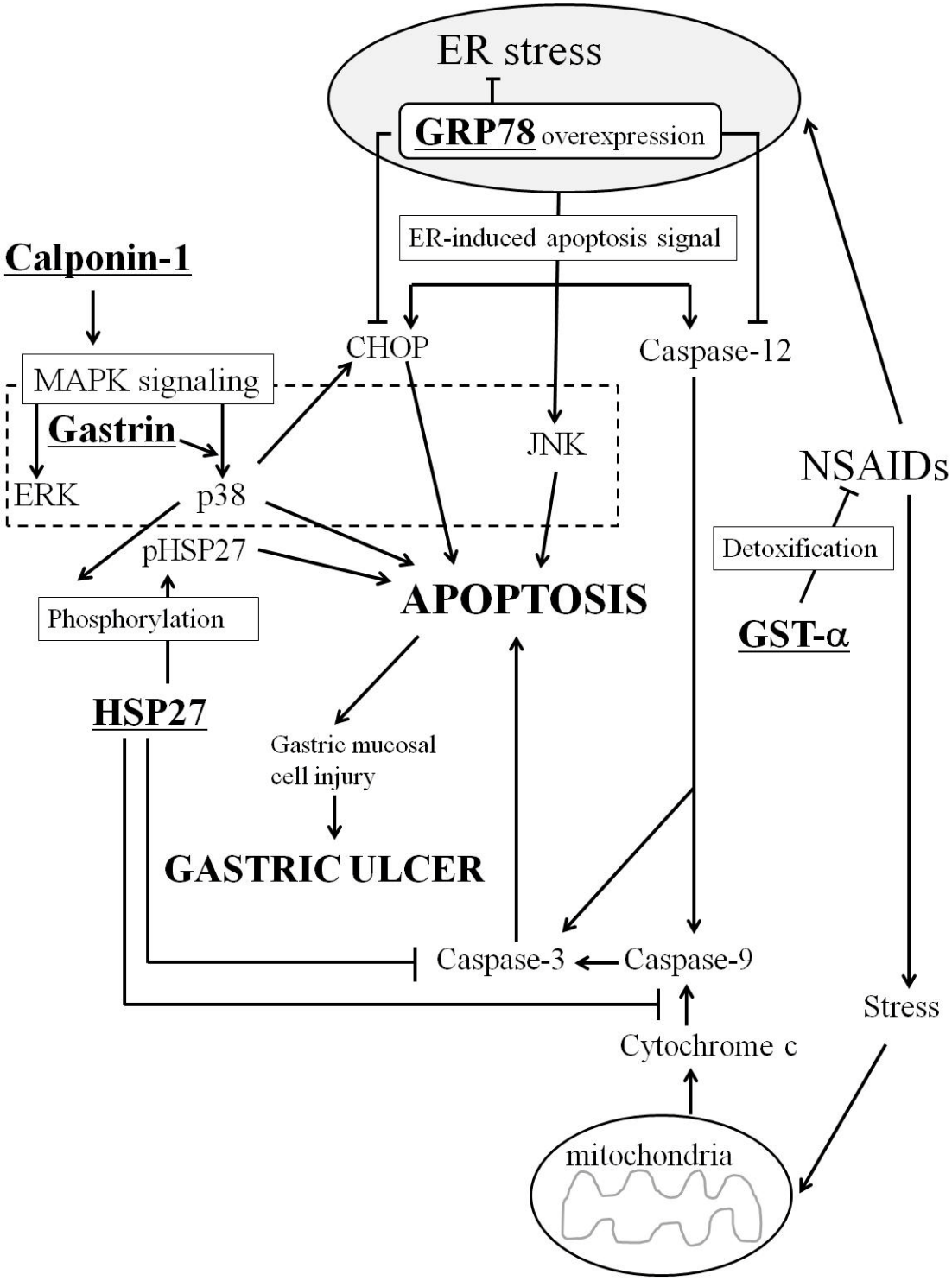
ER stress
GRP78 overexpression
ER-induced apoptosis signal
Calponin-1
CHOP
Caspase-12
MAPK signaling
Gastrin
JNK
NSAIDs
ERK
p38
pHSP27
Detoxification
APOPTOSIS
Phosphorylation
GST-α
HSP27
Gastric mucosal cell injury
GASTRIC ULCER
Caspase-3
Caspase-9
Stress
Cytochrome c
mitochondria